

Electronic coherences excited by an ultra short pulse are robust with respect to averaging over randomly oriented molecules as shown by singular value decomposition

Manuel Cardosa Gutierrez¹, R. D. Levine^{2,3,4}, F. Remacle^{1,2*}

¹Theoretical Physical Chemistry, UR MOLSYS, University of Liege, Belgium

²Fritz Haber Center, Institute of Chemistry, The Hebrew University of Jerusalem, Jerusalem 91904, Israel

³ Department of Molecular and Medical Pharmacology, David Geffen School of Medicine and

⁴Department of Chemistry and Biochemistry, University of California, Los Angeles, CA 90095, USA

Supplementary Information

Section S1: Singular value decomposition of the density matrix in the sudden approximation

Supplemental figures

Figure S1: Potential energy curves of the 7 lowest Σ states and 3 lowest Π states of the LiH molecule.

Figure S2: Selected electronic dipole curves.

Figure S3: Selected non adiabatic coupling (NAC curves) within the Σ manifold and the Π manifold.

Figure S4: Long time population dynamics for Π states for the 4.35 eV exciting pulse.

Figure S5: Orientation singular vector, \mathbf{V}_5 , computed at 18 fs for the dynamics induced by the 4.35 eV – 2fs pulse.

Figure S6: Relative errors on the populations of the electronic states computed by averaging of 800 initial random orientations and by the approximate SVD propagation scheme including the 5 largest principal components for the 4.35 eV – 2fs pulse.

Figure S7: Comparison between the time evolution of the populations of the electronic states computed by averaging of 800 initial random orientations and by the approximate SVD propagation scheme for the 4.35 eV – 2fs pulse.

Figure S8: Relative errors on the populations computed at 18 fs with 5, 8, 10, 12 and 15 σ_m for the 4.35 eV – 2fs pulse.

Figure S9: Frobenius distance between the density matrix averaged of 800 initial random orientations and the one approximated with 5 σ_m computed at 18 fs for the 4.35 eV – 2fs pulse and the 5.17 eV one.

Figure S10: Principal values, error on the norm, Δ_{Nmin} , and errors on the populations in the electronic states computed with 5 σ_m for the dynamics induced by the 2f 5.17 eV pulse.

Figure S9: Heatmaps of the orientation singular vectors corresponding to the 5 largest σ_m computed at 18 fs for the 5.17 eV – 2fs pulse.

Figure S11: Localization of the principal molecular vectors on the nuclear grid and on the adiabatic electronic states for the 5.17 eV – 2fs pulse.

Figure S12: Localization of the principal orientation vectors on the unit sphere for the 5.17 eV – 2fs pulse

Figure S13: Convergence of the emission dipole moment computed with 5 and 10 principal values for the 5.17 eV – 2fs pulse.

Figure S14: Real part of the electronic coherences for a 2fs- 4.35 eV pulse polarized in the (x,z) plane for a LiH molecule oriented as in Figure S1.

Figure S15: Heatmaps of the real part of the reduced nuclear density matrix computed for a 2fs- 5.17 eV pulse.

*Corresponding author: fremacle@uliege.be

Section S1: Singular value decomposition of the density matrix in the sudden approximation

In the sudden approximation for the photoexcitation, i.e. a one photon transition at t_p when the pulse is maximum, Eq. (4) of the main text, and restricting the dynamics to the excited states, the initial amplitudes at each point of the nuclear grid in each excited state can be factorized as the scalar product of the orientation of the electric field, $\hat{\mathbf{e}}_o$, and the transition dipole moment from the ground electronic state $\boldsymbol{\mu}_{GS-gi}^T = (\mu_{GS-gi}^x, \mu_{GS-gi}^y, \mu_{GS-gi}^z)$:

$$c_{gi}^0 = \hat{\mathbf{e}}_o^T \boldsymbol{\mu}_{GS-gi} \quad (\text{S1})$$

Then each element of $\rho^{mol}(t_p)$ are given

$$\begin{aligned} \rho_{gi,g'j}^{mol}(t_p) &= (1/N_o) \sum_o^{N_o} \left(\hat{\mathbf{e}}_o^T \boldsymbol{\mu}_{GS-gi} \right) \left(\hat{\mathbf{e}}_o^T \boldsymbol{\mu}_{GS-g'j} \right)^\dagger = \sum_o \left(\boldsymbol{\mu}_{GS-g'j}^T \cdot \hat{\mathbf{e}}_o \right) \left(\hat{\mathbf{e}}_o^T \boldsymbol{\mu}_{GS-gi} \right) \\ &= \boldsymbol{\mu}_{GS-g'j}^T \left(\sum_o \hat{\mathbf{e}}_o \hat{\mathbf{e}}_o^T \right) \boldsymbol{\mu}_{GS-gi} \end{aligned}$$

where $\sum_o^{N_o} \mathbf{e}_o^T \mathbf{e}_o = \begin{pmatrix} 1 & 0 & 0 \\ 0 & 1 & 0 \\ 0 & 0 & 1 \end{pmatrix}$ for an ensemble of random orientations. In that particular case,

$\rho^{mol}(t_p)$ is given by

$$\rho^{mol}(t_p) = \boldsymbol{\mu} \boldsymbol{\mu}^T \quad (\text{S2})$$

where the $((N_e-1) \times N_g) \times 3$ matrix $\rho^{mol}(t)$ is the matrix of the cartesian components of transition dipole between the GS and the excited states at each grid point. $\rho^{mol}(t_p)$ is independent of the polarization direction of the electric field of the pulse for an ensemble of randomly oriented molecules. It can only have 3 principal components oriented along the three cartesian axis of the molecular frame.

In the case of a sudden process, the matrix $\rho^{orien}(t_p) = \mathbf{A}^\dagger \mathbf{A}$ also takes a factorizable simple form. A matrix element of $\rho^{orien}(t_p)$ is given by

$$\begin{aligned}
\rho_{oo'}^{orien}(t_{exc}) &= \sum_{gi=1}^{Ne-1Ng} (c_{gi}^o)^* c_{gi}^{o'} = \sum_{gi=1}^{Ne-1Ng} (\hat{\mathbf{e}}_o^T \cdot \boldsymbol{\mu}_{GS-gi})^T (\hat{\mathbf{e}}_{o'}^T \cdot \boldsymbol{\mu}_{GS-gi}) \\
&= \sum_{gi=1}^{Ne-1Ng} \boldsymbol{\mu}_{GS-gi}^T \mathbf{e}_o \mathbf{e}_{o'}^T \boldsymbol{\mu}_{GS-gi} = \mathbf{e}_o \mathbf{e}_{o'}^T \sum_{gi=1}^{Ne-1Ng} \boldsymbol{\mu}_{GS-gi}^T \boldsymbol{\mu}_{GS-gi}
\end{aligned} \tag{S3}$$

each matrix element of $\rho^{orien}(t_{exc})$ will be multiplied by the same number which is the total oscillator strength. Using the $N_o \times 3$ matrix \mathbf{e} of the Cartesian components of the orientations $\hat{\mathbf{e}}_o$, defined above

$$\rho^{orien}(t_p) = \left(\sum_{gi}^{Ne-1Ng} \mu_{GS-gi}^2 \right) \mathbf{e} \mathbf{e}^T \tag{S4}$$

$\rho^{orien}(t_p)$ will therefore have 3 principal components oriented along the three cartesian axis.

It is not diagonal because the scalar product $\hat{\mathbf{e}}_o \hat{\mathbf{e}}_{o'}^T$ can be very close to 1.

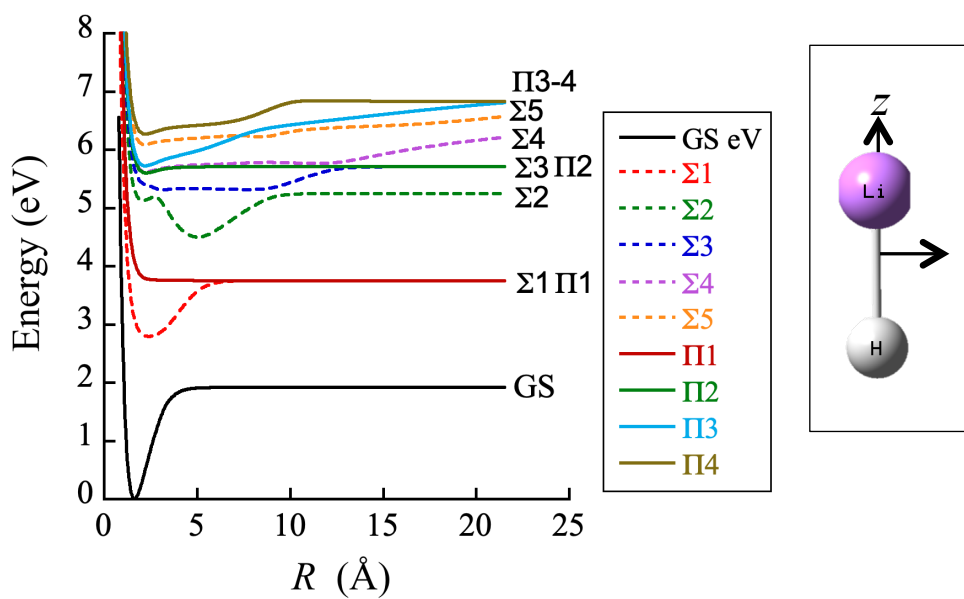


Figure S1: Potential energy curves of the 6 lowest Σ and the 4 lowest Π electronic states, adapted from ref [1]. Right: Orientation of the LiH molecule in the Cartesian molecular frame.

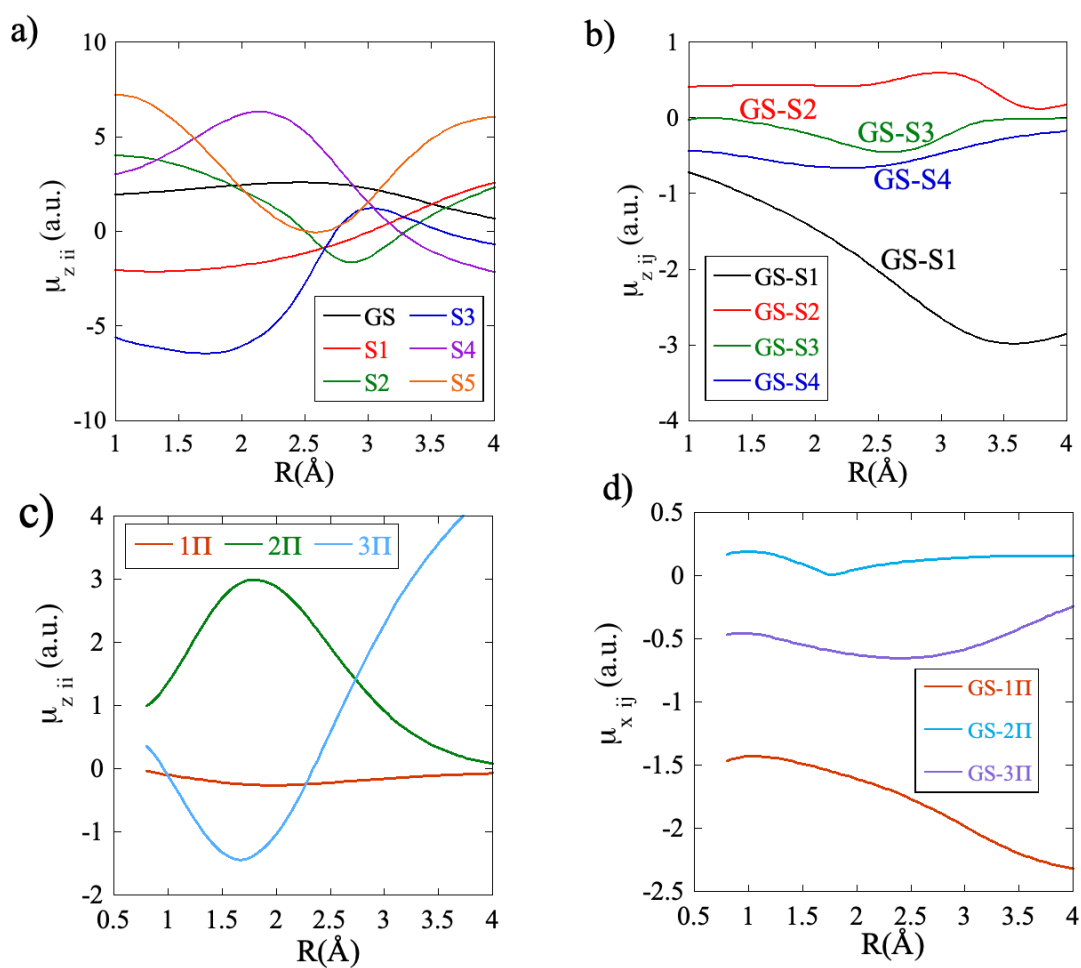


Figure S2: Selected electronic dipole curves for the Σ manifold (along z) a) permanent b) transition, c) and d) Π manifold permanent (along z) and transition (along x) respectively, adapted from ref. [1]. The values for the y components of the Π are identical.

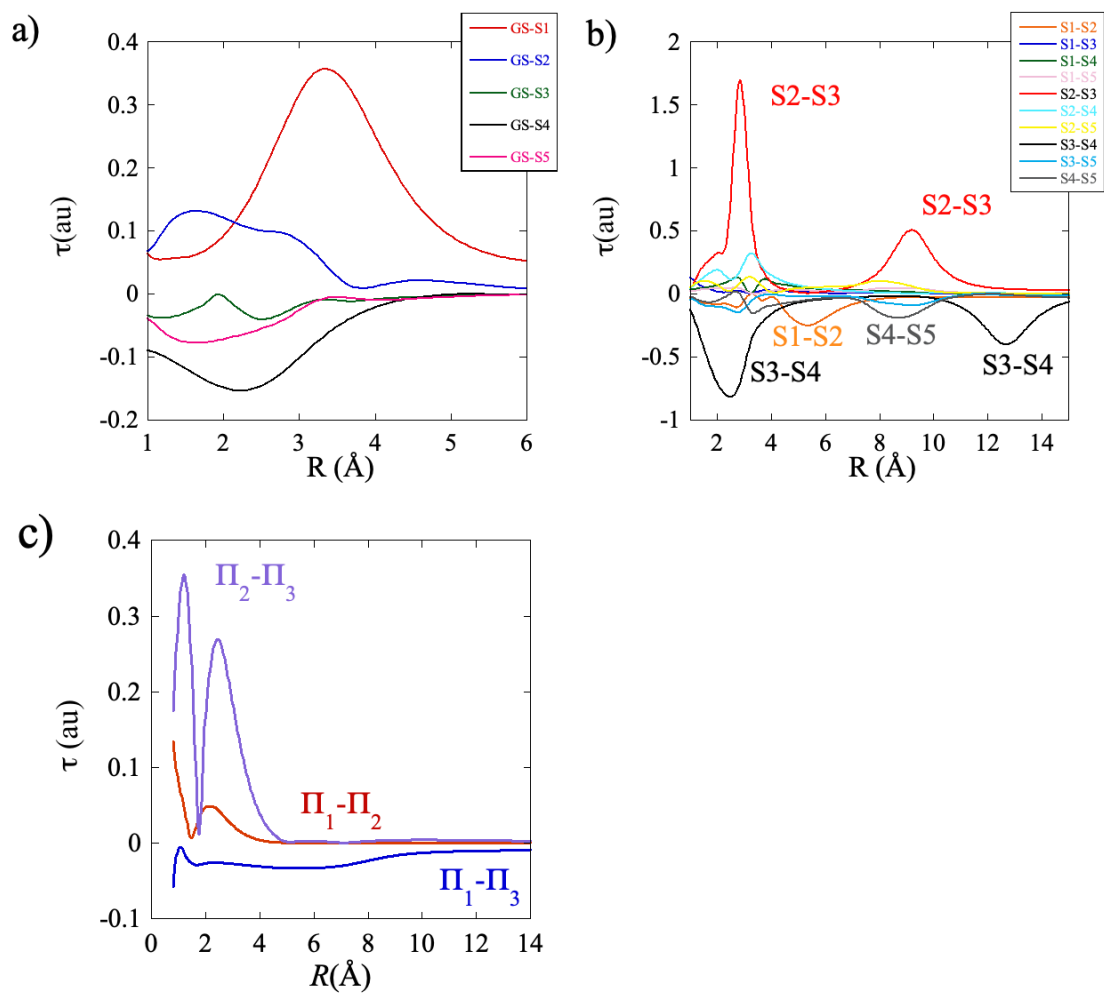


Figure S3 : Selected NAC curves a) Ground state to Σ excited states at short distance. b) Between Σ excited states, c) Between Π excited states, adapted from ref.[1].

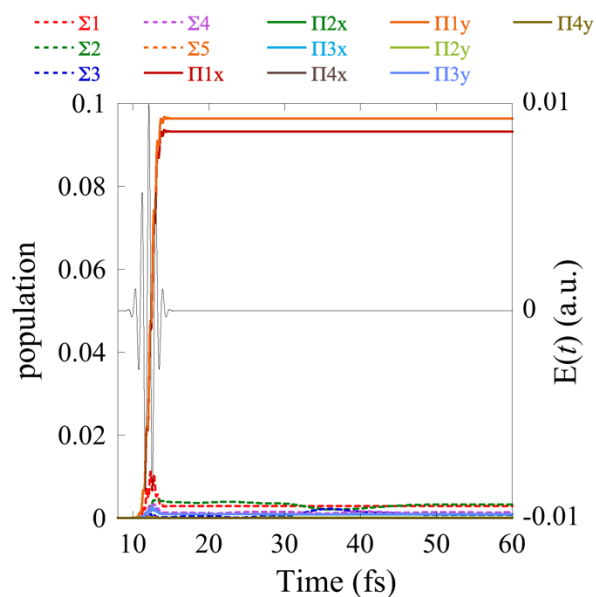


Figure S4. Long time dynamics in LiH for the two components of the Π_1 state computed for the 4.35eV-2fs exciting pulse, average over 800 initial random orientations. See Figure 1b for the details of the population in the Σ excited states.

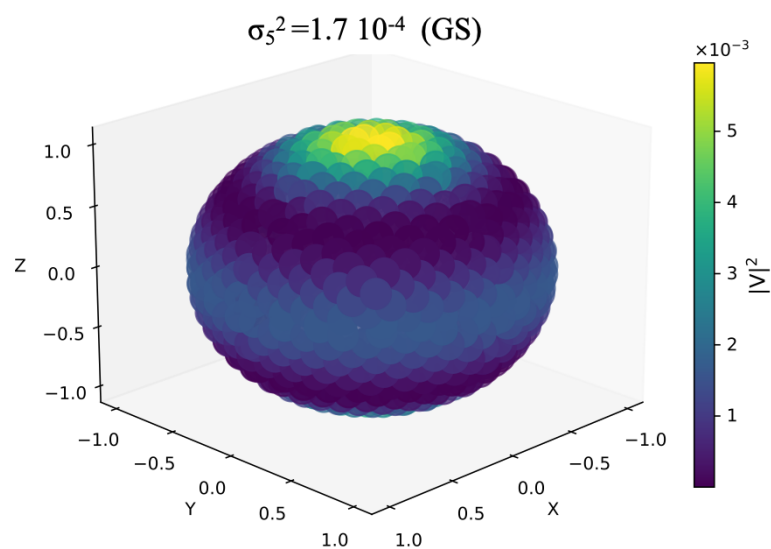


Figure S5. Localization of the \mathbf{V}_5 orientation on the sphere. It is oriented along z and localized on excited state of the GS (see Figure 4). Computed at 18 fs for the 4.35 eV – 2fs exciting pulse.

The relative error for the population of the GS and of the Π_1 state computed as an exact average over the 800 orientations or by the SVD propagation of the 5 largest principal components is of the order 10^{-4} percent (Figure S6a), which can be understood from the fact that 4 among the 5 principal values retained for the SVD propagation localize on these states. For the manifold of Σ_1 , Σ_2 , Σ_3 and Σ_4 (Figure S6b), the error is larger, of the order of a tenth of percent, which again can be understood from the fact that the population in those states is only ≈ 100 times larger than the threshold (10^{-5}) fixed to recover the trace of the ensemble density matrix and that only one singular component, the fourth one, accounts for the dynamics of the populations in the excited Σ manifold. The largest error is made when the non adiabatic coupling is strong between the excited Σ states. For completeness, we show in Figure S7 that the populations computed by the two methods cannot be distinguished to reading accuracy.

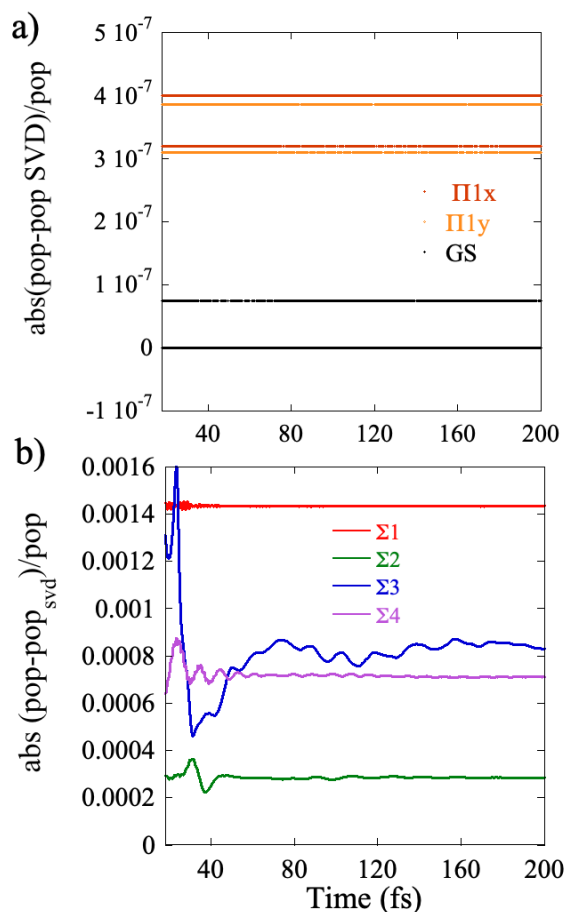


Figure S6. Relative errors on the populations of the GS and Π_1 states computed as an exact averaging over 800 initial orientations or by propagating the \mathbf{U}_m vectors of the 5 largest principal components. The plot of the populations is shown in Figure S6. Figure S7 of the SI shows the error on the populations at 18 fs computed for 5, 8, 10, 12 and 15 σ_m respectively.

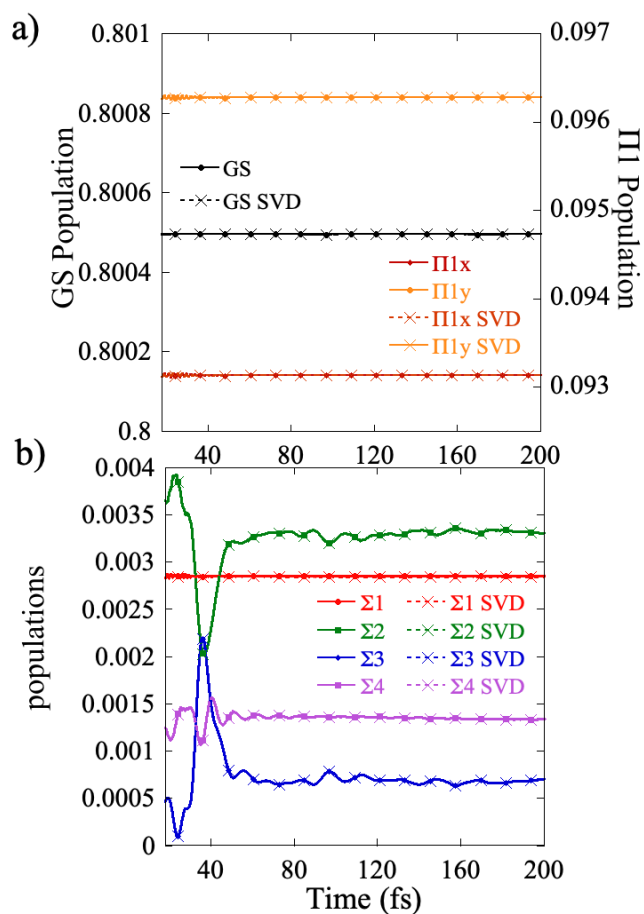


Figure S7. Comparison of the population in the electronic states for the excitation by the 4.35 eV – 2fs pulse, obtained by averaging the 800 randomly oriented initial states (full lines-full circles) and those computed using the five largest principal components of the SVD analysis (dotted lines, crosses). a) population in the two components of the Π_1 state and the GS. b) population in the manifold of Σ excited states.

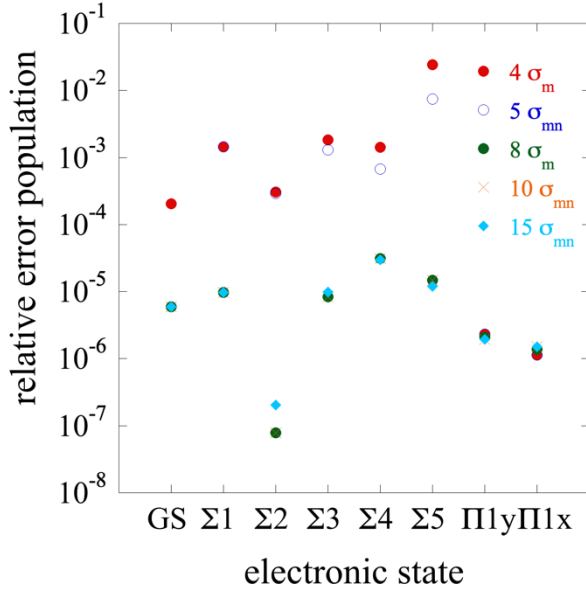


Figure S8: Error on the populations in the excited electronic states for excitation by the 4.35 eV- 2fs pulse computed at 18fs for an increasing number of principal components as indicated.

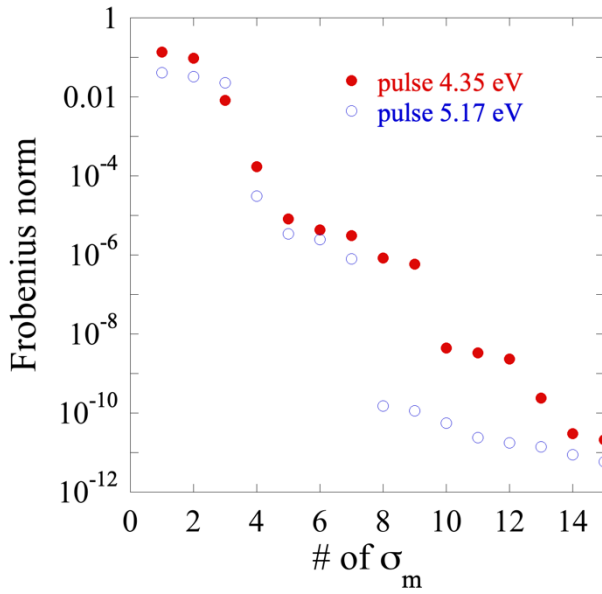


Figure S9 : Frobenius measure of the difference between the density matrix average of 800 initial orientations and the density matrix recovered with in increasing number of singular values computed at 18 fs, after the exciting pulse is over, for the two 2fs pulse used here with carrier frequencies of 4.35 and 5. 17 eV respectively. The Frobenius distance drops faster for the 5.17 eV pulse, with a gap at σ_8 . This pulse excites more commensurate populations in the excited Π and Σ manifolds. The Frobenius distance is computed as

$$\|F_m\| = \sqrt{\sum_{i=1}^N \sum_{j=1}^N \left| (\rho_{mol}^{av})_{ij} - (\rho_{mol}^m)_{ij} \right|^2} .$$

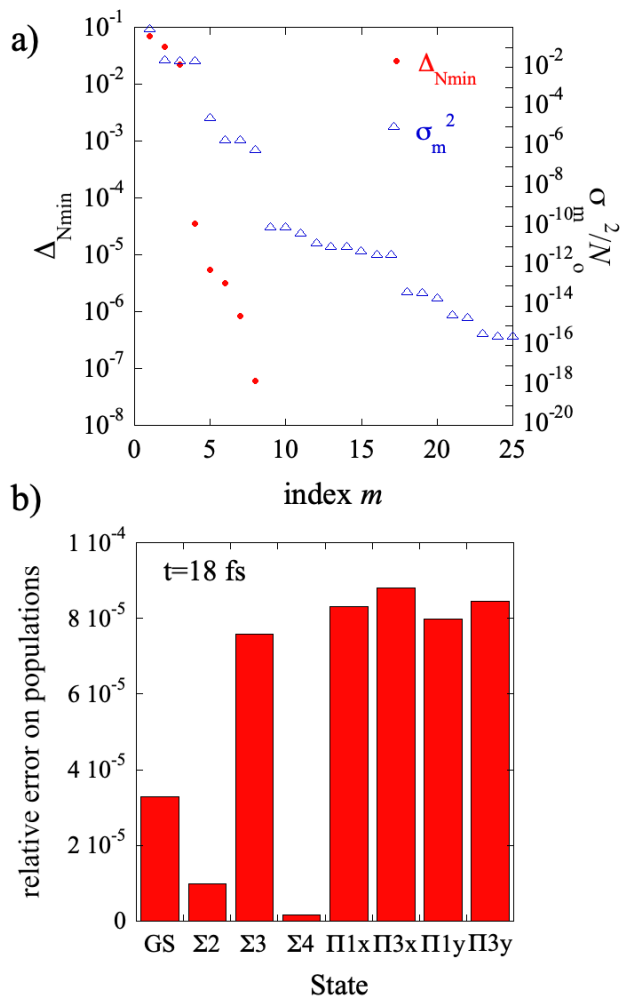


Figure S10. a) The normalized singular values, σ_m^2/N_0 , (right y axis) and Δ_{Nmin} (right axis) at $t=18$ fs, computed for the excitation of LiH by a 2fs deep UV pulse with a carrier frequency of 5.17 eV. Note the two breaks in the magnitude of the singular values, one between $m=4$ and $m=5$ and one between $m=8$ and $m=9$. The same break is obtained for the Frobenius distance shown in Figure S9. b) Relative error on the populations computed for 5 σ_m .

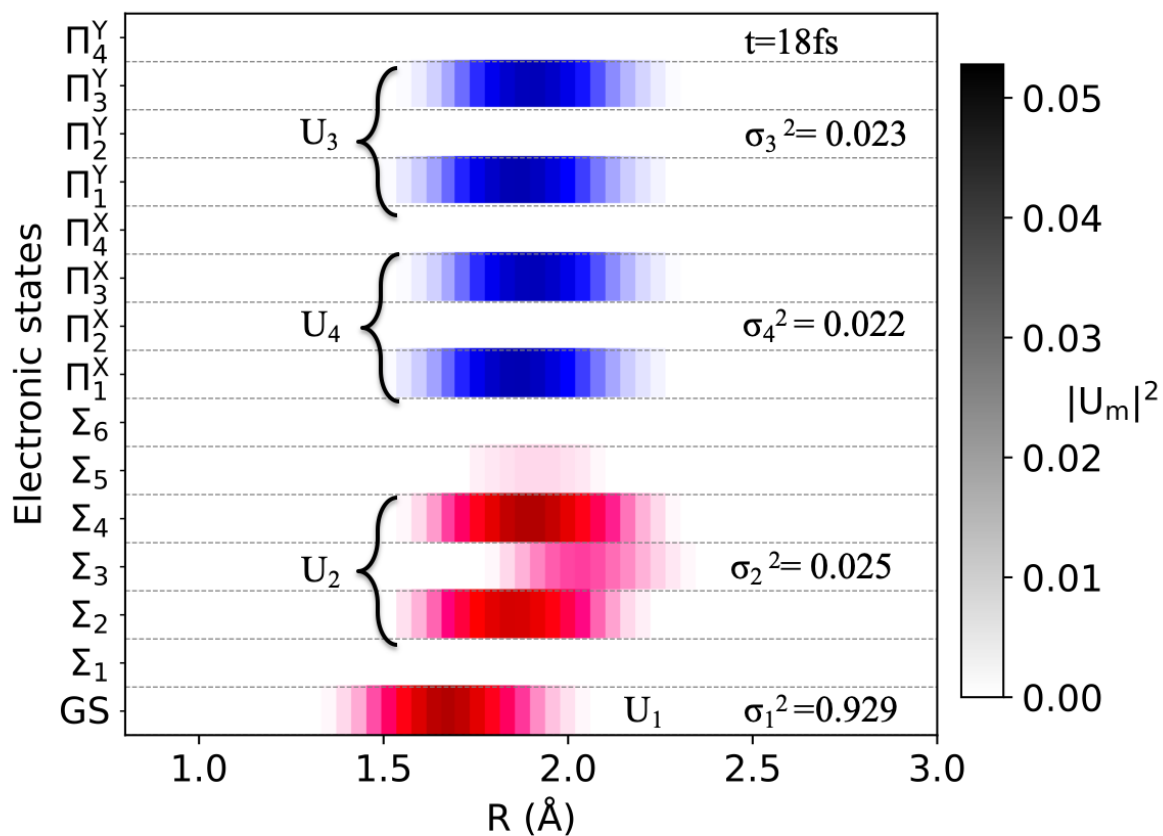
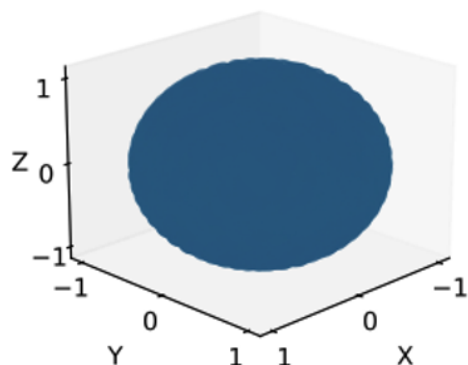
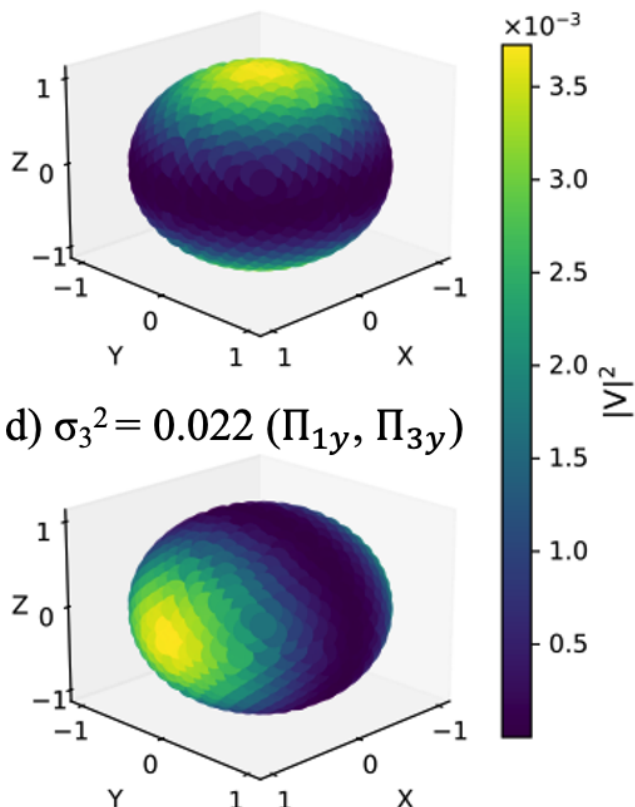


Figure S11: Heat map of the localization of the square modulus of the U_m vectors, $m = 1$ to 4, for the dynamics induced by the 2fs deep UV (5.17 eV) pulse at $t = 18$ fs, when the pulse is over.

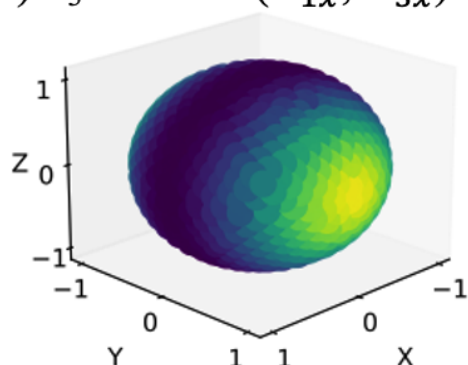
a) $\sigma_1^2=0.93$ (GS)



b) $\sigma_2^2=0.025$ (Σ excited states)



c) $\sigma_3^2=0.023$ (Π_{1x}, Π_{3x})



d) $\sigma_3^2=0.022$ (Π_{1y}, Π_{3y})

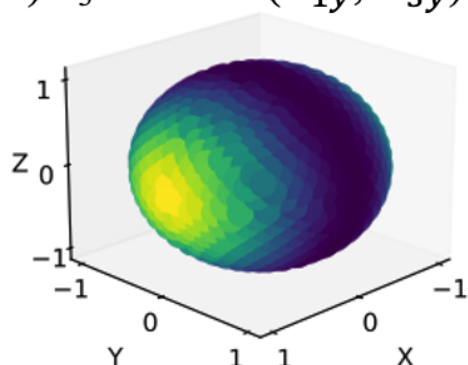


Figure S12. Heat map of the square modulus of the V_m orientation singular vectors that correspond to the four largest singular values computed at 18fs for an excitation by the 5.17 eV.

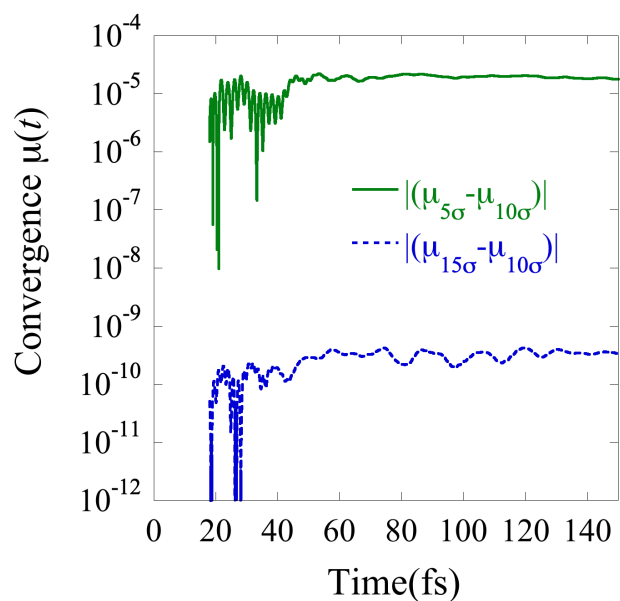


Figure S13. Convergence of the value of the time-dependent dipole, $\mu(t)$, for increasing number of principal components included in the propagation as indicated.

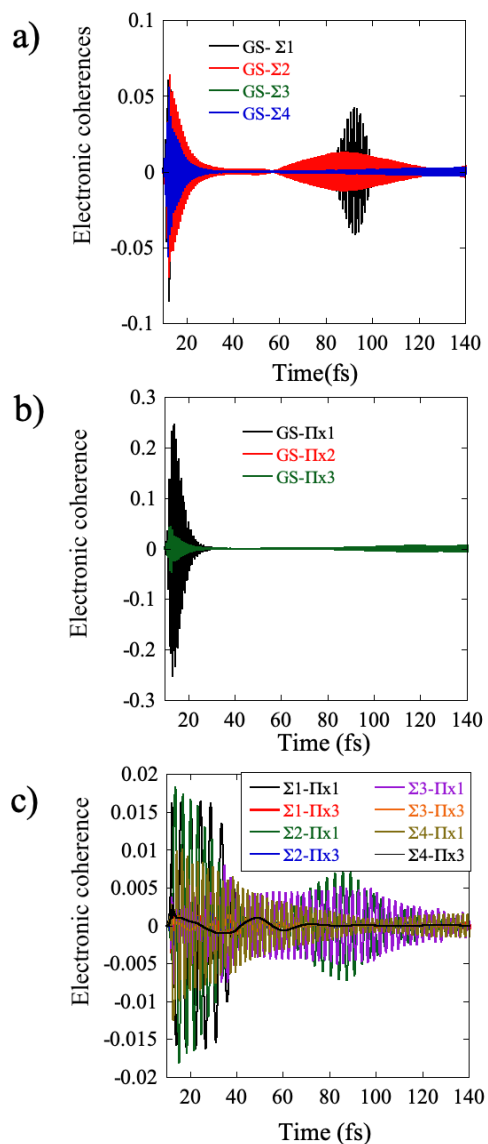


Figure S14. The Σ – Π electronic coherences that appear when the polarization direction of the pulse is in the (x,z) plane of the molecular frame for oriented molecules as shown in Figure S1. a) Electronic coherences between the GS of Σ symmetry and the excited Σ states. b) electronic coherences between the GS and the Π states. c) Electronic coherences between excited Σ and Π states. Not shown are the coherences within the manifold of excited Σ states and within the manifold of the excited Π states.

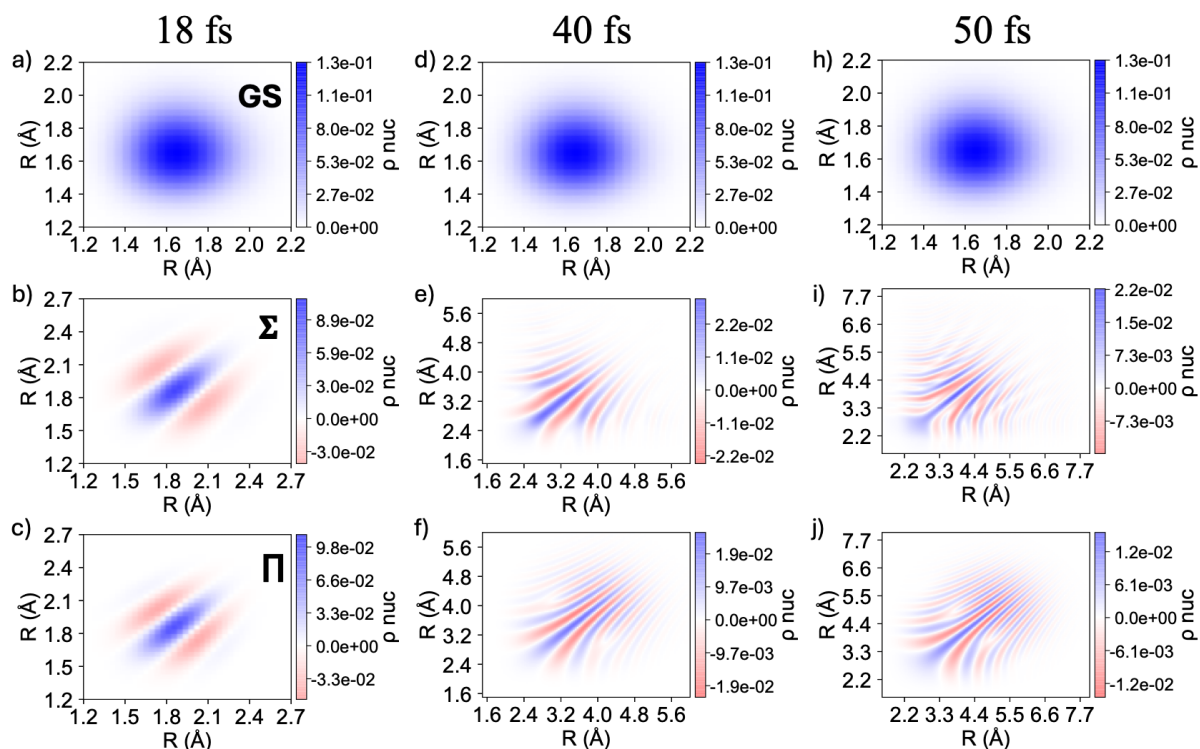


Figure S15: Heatmaps of the reduced nuclear density matrix, $\rho_{nuc,m}^{mol}(t)$ (Eq. (8) of the main text), for the 3 largest principal components of the ensemble dynamics induced by the higher frequency (5.17 eV) exciting pulse, computed at 18 fs (when the pulse is over), and 40 fs and 50 fs where there is a strong NAC coupling between the Π and the Σ states. Top row, $m=1$, localized on the GS, panels a),d),h). Medium row $m=2$, localized on excited Σ states, panels b), e), i). Bottom row, $m=3$, localized in Π states, panels c), f) and j). See figure S11 above. Note the effect of the NAC on the vibrational coherences of the third principal component, localized on Π states, at 40 and 50 fs.

Reference

[1]S. van den Wildenberg, B. Mignolet, R. D. Levine, and F. Remacle, J. Chem. Phys. **151**, 134310 (2019).